Identification and Optimization of Active Magnetic Bearing Systems Using Measured Nyquist Diagrams

Masujiro Hisatani

Machinery System Research Section, Tamano Laboratory
Mitsui Engineering and Shipbuilding
3-16-1, Tamahara, Tamano City, 706 JAPAN

Summary

An effective measurement and identification technique of the stability of active magnetic bearing systems is introduced. Frequency response is reduced into an open-loop transfer function and displayed as the Nyquist diagram. This shows the stability of the system both qualitatively and quantitatively. This technique is applied both for the axial direction, and for the radial direction with a strong gyroscopic effect. Measured Nyquist diagrams along the radial direction clearly show the divergence of eigenvalues caused by gyroscopic effect. A guide to optimize the system is indicated for the safe high speed rotation of the machine.

1. INTRODUCTION

The basic design of the control circuit of active magnetic bearing systems is simple: the main purpose is to overcome the negative stiffness of the rotor and afford an appropriate damping. In the case of a single degree of freedom (DOF) system, it is easily realized by PID control or phase-lead compensation. When a multi-DOF system has to be treated, it is described by state variable equations and techniques of either pole assignment or optimal regulator can be used.

However, actual tests often reveal the difference of the system characteristics with those of the design condition. It is usually worse than the designed one and sometimes the system becomes unstable. The causes of the system deterioration can be considered as frequency characteristics of the sensors, power amplifiers and control coils, incompletion of the compensation circuit, non-linearity of the magnetic attractive force characteristic, mechanical flexibility of the rotor, etc.

The most important "performance" of a control system is the stability. It is expressed by complex eigenvalues. A more elaborate model of the mechanical and electrical system than that of the design can be constructed to get complex eigenvalues closer to real values. However, it is difficult to model the frequency characteristic of every component accurately. Complex eigenvalues cannot be measured directly, but the performance can be measuered in the form of Nyquist or Bode diagrams. In order to investigate the actual system performance, impulse, step, or frequency response tests are often performed (1) (2) (3) and data are obtained in time or frequency domain. The obtained data are that of closed-loop and usually it is not easy to grasp the total system and get a good prospect to improve it adjusting parameters of the compensation circuit.

In this paper, an effective technique is introduced which measures and identifies the actual control system and directly shows the stability of the system as the Nyquist diagram.

2. EXPERIMENTAL APPARATUS

Fig.1 shows the vertical experimental apparatus of five-axis active control. A large hollow cylinder is connected to the top of a shaft and this causes a great gyroscopic effect. The rotor mass is about 3.4 Kg and the design rotational speed is 30,000 rpm. This is an elastic rotor with the first bending mode of 345 Hz. Radial displacement sensors of eddy current type are installed adjacent to radial coils. Sensor signals are input to analogue compensators and the outputs are sent to analogue power amplifiers of current feed-back type which energize control coils with currents proportional to the input signal up to a certain frequency range. A coordinate system with the origin at the center of the rotor mass is shown in Fig.2.

3. CONTROL SYSTEM OF AXIAL DIRECTION

Fig.3 is a block diagram of the control system and the measuring system of the axial direction, which is a single DOF

system independent of multi-DOFs of radial directions. G_R and Gc are the transfer functions of the rotor and the compensation circuit respectively, k_s the sensitivity of the displacement sensor, R_{PA} the equivalent resistance of the power amplifier, and k_i the current stiffness of the control coils. A test signal e_t is added to the displacement signal e_z and these signals are input to the FFT analyzer to obtain a closed-loop transfer function which is expressed as :

$$G_{CL} \equiv e_z/e_t = -k_s G_R k_i / R_{PA} \cdot G_c (e_z + e_t)/e_t$$

where e_z and e_t are assumed to be Laplace transformed.

The open-loop transfer function of the system is

$$G_{OL} \equiv k_s G_R k_i / R_{PA} \cdot G_c$$

Therefore G_{CL} and G_{OL} have the following relation.

$$G_{OL} = -G_{CL}/(1+G_{CL}) \qquad (1)$$

The analyzed result of G_{CL} is transferred from FFT to the personal computer and the open-loop transfer function G_{OL} is calculated using equation (1). This is displayed in a complex plane as a Nyquist diagram with frequency as a parameter. Stability is inspected by the turning mode of the curve around the point (-1,0).

Now G_{OL} is proportional to Gc, the compensator. Therefore, when the stability of the system is not sufficient and the gain and the phase of Gc has to be modified, it can be done more easily using the Nyquist diagram of G_{OL} rather than using the closed-loop G_{CL} which is not directly proportional to Gc.

Some examples of measured Nyquist diagrams are shown in Fig.4. Frequencies in Hz are indicated on the curves. Curves No.1 and 2 represent designed PD (proportional and differential) gains but with and without I(integral) action respectively. Both curves turn around the point (-1,0) looking to the left, so the system is stable with phase margins about 18 to 20 degrees. The initial part (near DC) of curve No.1 extends greatly upward and indicates enlarged static stiffness due to integral action.

However, the phase margin is about two degrees less than the non-integral curve of No.2. The basic characteristics of the curve has been explained in [4].

In order to express the system stability directly, the frequency and damping ratio of the eigenvalues is identified as follows. The components of the system are approximated simply as:

$$G_R(s) = 1/(m s^2 - k_d)$$
$$G_c(s) = k_P + k_D s + k_I / s$$

where s represents Laplace operator, m the rotor mass, and k_d the displacement stiffness. A rigid rotor and an ideal PID control with gains k_P, k_I and k_D respectively are assumed. The open-loop transfer function is then expressed as:

$$G_{OL}(s) = k_s k_i / R_{PA} \cdot (k_P + k_D s + k_I / s)/(m s^2 - k_d)$$

Let $s=j\omega$, then $G_{OL}(j\omega)$ approximates the measured diagrams in Fig.4. A curve-fitting least square method was used to identify the eigen-frequency and the damping ratio which is lead from the characteristic equation $1+G_{OL}=0$. TABLE 1 summarizes measured and identified results. The damping ratio of the original setting (No.1) is less than expected. Therefore the differential gain was almost doubled (No.3) and a satisfactory value for the damping ratio was obtained. A larger value of the differential gain brings noise and high frequency oscillation. The optimization of the system can be achieved through a trade-off of these effects using Nyquist diagrams.

4.CONTROL SYSTEM OF RADIAL DIRECTION

The equation of motion for a rigid rotor can be stated by four radial DOFs, x, y, θ_x, and θ_y as follows:

$$\left.\begin{aligned} m\ddot{x} &= k_d x + k_i i_x \\ m\ddot{y} &= k_d y + k_i i_y \\ J_r \ddot{\theta}_x + J_a \omega_R \dot{\theta}_y &= k_{dt} \theta_x + k_{it} i_{tx} \\ J_r \ddot{\theta}_y - J_a \omega_R \dot{\theta}_x &= k_{dt} \theta_y + k_{it} i_{ty} \end{aligned}\right\} \quad (2)$$

where Jr and Ja are the moment of inertia about the radial and axial directions respectively, ω_R the angular rotational speed, and i the control current.

The equations above indicates that the translations x and y are essentially independent and can be treated as single DOFs as well as z. On the other hand, rotational motion θ_x and θ_y are coupled with each other by the gyroscopic terms when the rotor is rotating. Thus the rotational motion is treated as one of two DOFs as shown by a block diagram of Fig.5. Here two kinds of compensation circuits are used : G_{MC}, main compensation and G_{xc}, cross compensation. $J_a \omega_R s$ represents gyroscopic terms.

Although the control system now seems much more complicated, the same simple measuring technique can be applied with a test signal e_t input to θ_y system, and the following transfer functions concerning θ_y are obtained:

$$G_{CL} \equiv \frac{e_{\theta y}}{e_t} = -\frac{G_{OL\theta}}{1+G_{OL\theta}} \Big/ \left[1+\left\{\frac{G_R(G_{XC}'+J_a\omega_R s)}{1+G_{OL\theta}}\right\}^2\right] \quad (3)$$

$$G_{OL} \equiv -G_{CL}/(1+G_{CL}) = G_{OL\theta} \Big/ \left[1+\frac{G_R^2(G_{XC}'+J_a\omega_R s)^2}{1+G_{OL\theta}}\right] \quad (4)$$

where

$$G_{OL\theta} = k_s k_i / R_{PA} \cdot G_R G_{MC}$$

$$G_{XC}' = k_s k_i / R_{PA} \cdot G_{XC}$$

The second term of the denominator represents the gyroscopic and cross compensation effect. Eq.(3) and (4) shows that, on the contrary to the simple case of axial direction, the control characteristics of the radial rotational motion changes greatly as the rotational speed of the rotor increases. This is clearly indicated by the measured data of Fig.6. In this case, PI control was used in the cross compensation G_{xc}. The lower frequency range of the diagrams indicates the effect of P control of G_{xc} which stabilizes precession, the lower eigenvalue diverged by the gyroscopic effect. At higher frequency range over 100 Hz the curve approaches (-1,0) as the rotational speed increases, indicating the decrease of stability of nutation, the higher branch of the eigenvalue.

This inclination of instability is caused by the phase lag of the main compensation circuit due to various kinds of filters

used. Fig.7 shows simulated curves corresponding to Fig.6, with low pass filters included in G_{MC} in eq.(4). The stabilization of precession and the destabilization of nutation are expressed. D control of the cross compensation must be useful for stabilizing nutation. But, in this case, it causes the onset of the oscillation of higher bending mode. Therefore a notch filter in the main compensation was used with a successful result shown in Fig.8, where f_N is the center frequency of the notch filter and k_N is the proportion of full filtering.

The eigenvalues of the bending mode are also diverged by the gyroscopic effect. Fig.6 shows the divergence of the first bending mode, which is originally located at 345 Hz, and diverges into 320 Hz and 410 Hz at 10,000 rpm. Care should be taken if these branched eigenvalues approach instability.

The measuring technique stated above guarantees a reliable observation of the system stability as the rotational speed increases, and ensures a safe high-speed rotation of the machine. Realistically suitable variable-gain control method will be realized using the result of optimization obtained. For elastic rotors this measuring technique could be expanded into a more precise form considering the variation of the transfer function with space and utilizing more information from additional displacement sensors.

5. CONCLUSION

(1) A simple and effective measuring technique was introduced which identifies the actual performance of the control system of active magnetic bearing systems and enables its optimization. The result is displayed as a Nyquist diagram.

(2) The method is applicable not only for a simple case of single DOF but also for multi DOFs having coupled terms such as gyroscopic terms. The measured Nyquist diagram clearly indicates the gyroscopic effect which diverges system eigenvalues of both the rigid mode and of the bending mode.

Acknowledgement

The author wishes to express his appreciation to Mr. S. Nakata and Mr. K. Nakamura for their assistance, and is grateful to Mitsui Engineering and Shipbuilding for the permission to present this paper.

References

1. Humphris,R.R.,Allaire,P.E.,et al:Effect of Control Algorithms on Magnetic Journal Bearing Properties. J. of Eng. for Gas Turbines and Power Vol.108,No.4 October 1986

2. Bradfield,C.D.,Roberts,J.B.,Karunendiran,R.:Performance of an electromagnetic bearing for the vibration control of a super-critical shaft. PIME Vol.201,No.C3,1987

3. Hisatani,M., Inoue,Y., Mitsui,J.: Development of digitally controlled magnetic bearing. Bulletin of JSME Vol.29 No.247 January 1986

4. Kamerbeek,E.M.H.: Magnetic bearings. Philips Tech.Rev.41, 1983/84,No.11/12

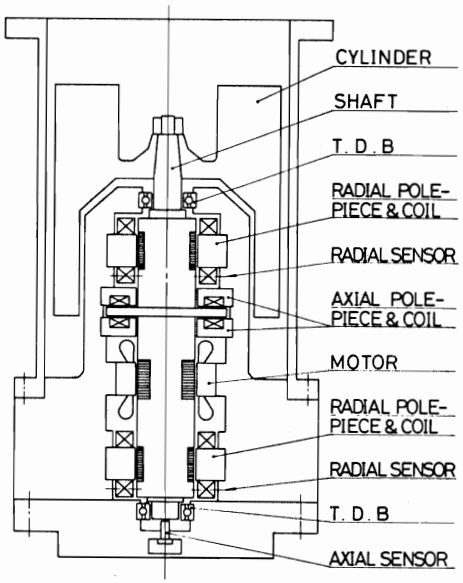

Fig.1 Experimental apparatus

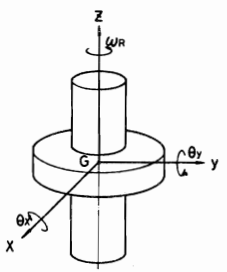

Fig.2 Co-ordinate system

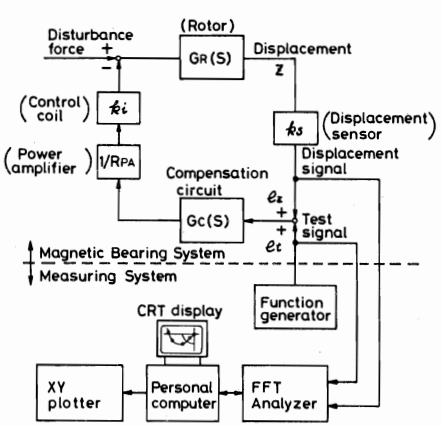

Fig.3 Control system & Measuring System (axial direction)

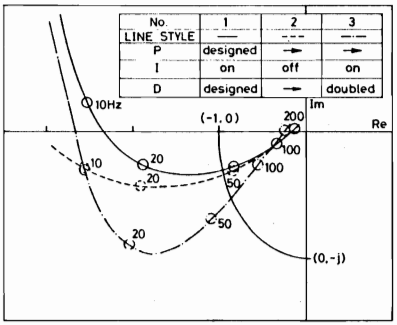

Fig.4 Measured Nyquist diagram (axial direction)

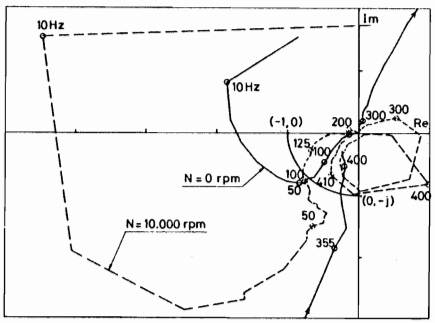

Fig.6 Measured Nyquist diagram of θy direction

No.	1	2	3
Measured Phase margin	18°	20	30
Identified eigenfrequency	42Hz	42	37
damping ratio	0.24	0.26	0.58

TABLE 1 Identification of eigenvalues

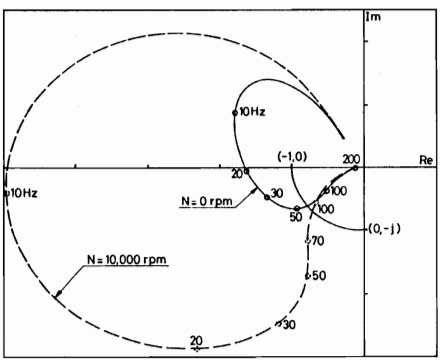

Fig.7 Simulated Nyquist diagram of θy direction

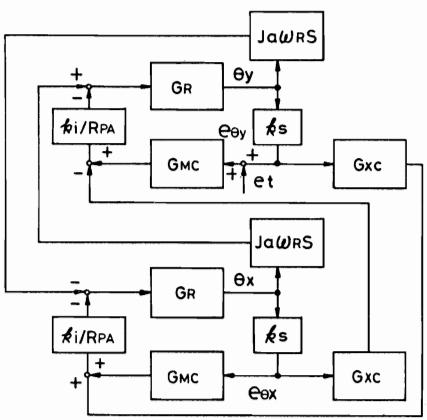

Fig.5 Control system of radial rotational motion

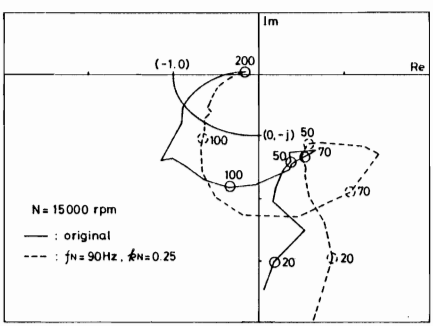

Fig.8 Effect of notch filter on the stability of nutation